



Cross-section stability of hot-rolled and welded I-shapes under combined loading

Liya Li¹, Lucile Gérard², Nicolas Boissonnade³

Abstract

This paper investigates the resistance capacity of hot-rolled and welded I-sections subjected to combined loading as influenced by plasticity and local buckling effects. Extensive numerical parametric studies through validated finite element models were carried out to consider different steel grades, section shapes and various load cases including bi-axial bending without axial compression (M_y+M_z), mono-axial bending with axial compression ($N+M_y$ or $N+M_z$) and bi-axial bending with axial compression ($N+M_y+M_z$). Based on the Overall Interaction Concept (O.I.C.), a three-dimensional resistance space was built to capture the cross-section behaviour under different load cases and interaction design equations are proposed, based on the numerical results. Overall, it is evidenced that the proposed O.I.C approach provides more continuous and significantly more accurate resistance predictions than existing design standards.

1. Introduction

The use of steel components in construction remains a quite popular structural solution, especially through the use of open sections, like hot-rolled and welded I and H-sections, which are mainstream section types in steel structures. Owing to steel outstanding resistance and structural performance, the design of steel elements shall properly address instabilities under compressive stresses and various buckling modes. The latter becomes more complex when considering combined load cases, as a result of many parameters influencing the section's response. Since combined load cases are far from uncommon in steel construction, the need for a sound-based, meaningful yet simple and accurate design approach is obvious.

Combined load cases have usually been studied through so-called “beam-column” problems. The structural response, behaviour and design of steel I-shaped beam-columns are complex and difficult problems within Structural Engineering. In this paper, the (local) section behaviour is considered, which therefore eliminates global instability modes such as flexural buckling and/or lateral torsional buckling (L.T.B.).

A significant number of researchers have tackled the steel beam-column problem, and an important amount of literature can be found on this topic, so that it is vain to provide an exhaustive summary. Among these, an early attempt can be found dating back to the 1970s by

¹ Ph.D., Laval University, <liya.li.1@ulaval.ca>

² Ph.D., Laval University, <lucile.gerard.1@ulaval.ca>

³ Professor, Laval University, <nicolas.boissonnade@gci.ulaval.ca>

(Massonnet, 1976), which can be considered the first milestone reference on the topic as an extensive state-of-the-art. Many other authors have investigated further the beam-column problem and provided improved design rules, such as (Boissonnade et al., 2006; Chen and Atsuta, 1977; Galambos, 1998; Jaspart et al., 1993; Maquoi et al., 2001; Ofner, 1997). Several of the latter research works have been considered for implementation in design standards; although a significant amount of knowledge is available on the matter, several problems still remain within standards when focusing on section resistance.

Current design codes continue to be predominantly based on numerous experimental practices and rely on mechanical bases as much as possible. However, according to the deficiencies mentioned in (Boissonnade et al., 2006; Nseir, 2015), the Effective Width Method (E.W.M.) adopted in current design standards, such as in EN 1993-1-5 (EN 1993-1-5, 2006) and in the American Specifications AISC-360 (AISC, 2010), results in long and tedious design calculations for the cross-section effective properties. Furthermore, it is observed that most of the classification approach in current standards is mainly made for simple load cases so that practical difficulties often arise from the use of section classification when it comes to combined load cases such as $N+M_z$, M_y+M_z or $N+M_y+M_z$ (Chen et al., 2013). Especially for the M_y+M_z case, disproportionate efforts between the classification step and the following design checks are regularly met in practice. Furthermore, several inconsistencies still remain in current codes. For example, cross-section resistance is usually calculated irrespective of the section's production process, hot-rolling or plate welding, while it is well-known that welded residual stresses are usually quite higher and influence the resistance of compact to semi-compact sections. Likewise, the beneficial effect of plate interactions within the section are often neglected, and so are post-buckling reserves (Nseir, 2015). Especially for combined loading cases, interaction curves designed for slender sections which rely on verification against yield criterion and E.W.M. exhibit inaccuracies, inefficiency and are usually quite conservative. More details on specific design rules such as Eurocode 3 and the American Specifications are detailed in Section 2.

In recent years, Kettler (Kettler, 2008) carried out several experimental tests to study the cross-section resistance of Class 3 hollow and open sections and proposed a smooth, linear resistance transition from Class 2 (plastic) to Class 3 (semi-compact) sections. Because the plastic criterion is key to verifying the section's resistance in current standards, Baptista (Baptista, 2012) suggested simplified interaction criteria for I-sections subjected to compression with biaxial bending moments, for both elastic limit states and plastic limit states. These criteria were then compared with Eurocode 3 recommendations and proved that the Eurocode rules are usually conservative. Gkantou et al. (Gkantou et al., 2017) studied the section behaviour of hot-rolled high-strength steel hollow sections subjected to axial compression and uniaxial bending. They showed that interaction curves in Eurocode 3 usually provide safe predictions for Class 1 and 2 sections and that the E.W.M. is still applicable to high-strength steel hollow sections. Liew and Gardner (Liew and Gardner, 2015) investigated all combinations of axial load and bending moments for box sections and I-sections and extended the Continuous Strength Method (C.S.M.) to combined load cases. The design equations proposed are of a similar but more complex format compared with the interaction formula suggested in Eurocode 3. Following these investigations, Yun et al. (Yun et al., 2018a) conducted a series of experimental tests on hot-rolled stocky I-sections subjected to mono-axial and bi-axial eccentric compression. Zhao et al. (Zhao et al., 2015a) carried out an experimental programme to investigate the cross-sectional behaviour of stainless steel hollow sections under combined loading which covers both austenitic and duplex stainless steels. In addition, they simplified the equation for cross-sections proposed by (Liew and Gardner, 2015) and improved the interaction expressions of Eurocode 3 by changing end points with C.S.M. simple loading expressions (Yun et al., 2018b;

Zhao et al., 2015b), which are now extended to stainless steel channel sections (Liang et al., 2019a; Liang et al., 2019b; Liang et al., 2020) and stainless steel welded I-sections under minor-axis combined loading (Sun et al., 2021). In 2017, Arrayago et al. (Arrayago et al., 2017) studied the section behaviour of several stainless steel hollow sections subjected to combined compression and uniaxial bending and proposed a Direct Strength Method (D.S.M) to predict the section's capacity by modifying the approach developed by (Rasmussen, 2006) for beam-columns.

Besides, an alternative design philosophy, the Overall Interaction Concept (O.I.C.), has been developed in recent years to address several of the shortcomings detailed previously. The O.I.C., which is based on the well-established resistance-instability interaction with a definition of generalised relative slenderness, abandons the cross-section classification concept and the E.W.M. and deals with all cross-section shapes in a similar way for both sections and members, under simple or combined loading cases – more details about the O.I.C. will be given in Section 2.3.

This paper aims at extending the O.I.C. approach to the design of hot-rolled and welded I-sections under combined load cases. These research works were carried out based on validated F.E. models and then used for extensive numerical studies, for analyzing the influence of various key parameters and for deriving suitable O.I.C.-based design equations. Firstly, a review of current design rules for combined loading situations is described in Section 2. Then, the details of numerical models as well as validation results are provided in Section 3. On the basis of the validated F.E. models, extensive numerical parametric studies were carried out in Section 4 to consider different steel grades, section shapes and various load cases including bi-axial bending without axial compression (M_y+M_z), mono-axial bending with axial compression ($N+M_y$ or $N+M_z$) and bi-axial bending with axial compression ($N+M_y+M_z$). Through a design methodology based on the O.I.C., a three-dimensional resistance loading space was built (Section 5) to capture the cross-section behaviour under different load cases, and subsequent design equations are proposed. Section 6 compares the accuracy and performance of the proposed approach to the reference numerical results, as well investigates its benefits with respect to existing design rules.

2. European and American design rules for combined loading situations

2.1 Eurocode EN 1993-1-1 (EC 3)

To estimate the local resistance of steel sections, most of current design codes (AISC, 2010; EN 1993-1-1, 2005) rely on the concept of cross section classification, which separates cross sections into several classes according to their rotational capacity and their sensitivity to local buckling, as based on a measure of plates' slenderness. Table 1 summarizes the concept of section classification according to Eurocode 3 and relates Class to response and resistance of the section – from plastic and ductile (high rotational capacity) to slender and effective resistance. For example, plastic sections are classified as Class 1-2, while slender sections are classified as Class 4 in Eurocode 3 (EN 1993-1-1, 2005).

Table 1. Section classes according to the European Standards (Eurocode 3).

Class	1	2	3	4
<i>Response</i>	Plastic, high ductility	Plastic, limited ductility	Elastic-plastic	Slender, local buckling
<i>Resistance</i>	$M_{Rd} = W_{pl} \cdot f_y$	$M_{Rd} = W_{pl} \cdot f_y$	$M_{Rd} = W_{ep} \cdot f_y$	$M_{Rd} = W_{eff} \cdot f_y$

Usually, no difference between hot-rolled and welded sections is prescribed in typical design equations at the cross-section level. For Class 1 and Class 2 sections acted by a combination of axial force and biaxial bending, Eurocode 3 prescribes a strength check as defined by Eq. (1),

where $M_{y,Ed}$ and $M_{z,Ed}$ correspond to the applied major and minor-axis bending moments, respectively, and $M_{N,z,Rd}$ and $M_{N,y,Rd}$ are functions of their associated plastic bending resistances as influenced by axial compression; α and β are coefficients associated mainly to the relative level of axial compression and the section's shapes (i.e., open section or hollow section shape).

$$\left[\frac{M_{y,Ed}}{M_{N,y,Rd}} \right]^\alpha + \left[\frac{M_{z,Ed}}{M_{N,z,Rd}} \right]^\beta \leq 1 \quad (1)$$

$$W_{ep} = W_{pl} - (W_{pl} - W_{el})\beta_{ep} \quad (2)$$

For combined loading situations, elastic-plastic bending resistances $M_{ep,y,Rd}$ and $M_{ep,z,Rd}$ shall be used within Eq. (1), in replacement of $M_{N,y,Rd}$ and $M_{N,z,Rd}$, respectively. Nevertheless, α and β factors are kept identical to Class 1 and 2 cases, maintaining discontinuities from plastic to elastic resistances along the Class 3 range, and in particular at the Class 3-4 limit.

The resistance of Class 4 sections under combined compression and biaxial bending is restricted to the elastic strength of sections, “penalized” by the presence of (imaginary) holes where local buckling is deemed most severe, according to the bases of the E.W.M. This requires further calculation steps which makes the design process more time-consuming. The design check suggested by Eurocode 3 (Eq. (3)) necessitates the determination of (i) effective properties for each individual load case and of (ii) the distribution of stresses from possible additional bending moments induced by eccentricities e_{Ny} and e_{Nz} caused by a centroidal shift under the axial force. In Eq. (3), A_{eff} , $W_{eff,y}$ and $W_{eff,z}$ are effective properties calculated through the Effective Width Method. The implementation of the E.W.M. in Eurocode 3 can be shown inconsistent with the classification system since the latter is based on the so-called “original Winter formula” (EN 1993-1-1, 2005), while the E.W.M. is based on the “modified Winter formula” (EN 1993-1-5, 2006; Johansson et al., 2007).

$$\frac{N_{Ed}}{A_{eff}f_y} + \frac{M_{y,Ed} + N_{Ed}e_{Ny}}{W_{eff,y}f_y} + \frac{M_{z,Ed} + N_{Ed}e_{Nz}}{W_{eff,z}f_y} \leq 1 \quad (3)$$

2.2 American Standards AISC 360-10 (A.I.S.C.)

Compared with Eurocode 3, the American Standards (AISC, 2010) do not apply a single, consistent, and simple approach: each situation has a different set of design recommendations, usually based on the classification of the plates comprised within the cross-section. For Class 1-2 sections, i.e., compact sections, $M_{c,Rd,y}$ and $M_{c,Rd,z}$ are their corresponding plastic bending resistances; for Class 3 sections, i.e., non-compact sections, a linear transition between plastic bending resistances and elastic bending resistances is applied; for Class 4 sections, i.e., slender sections, the relevant compression and bending resistances are calculated through effective properties. The U.S. Standards also apply interaction formulae for members under combined loading, as shown in Eqs. (4) and (5) where $N_{c,Rd}$, $M_{c,Rd,y}$ and $M_{c,Rd,z}$ are the axial and flexural member strengths. It shall finally be noted that like Eurocode 3, hot-rolled and welded sections shall be designed with the same set of equations and parameters, regardless of the manufacturing process.

$$\text{When } \frac{N_{Ed}}{N_{c,Rd}} \geq 0.2 \quad \frac{N_{Ed}}{N_{c,Rd}} + \frac{8}{9} \cdot \left(\frac{M_{y,Ed}}{M_{c,Rd,y}} + \frac{M_{z,Ed}}{M_{c,Rd,z}} \right) \leq 1 \quad (4)$$

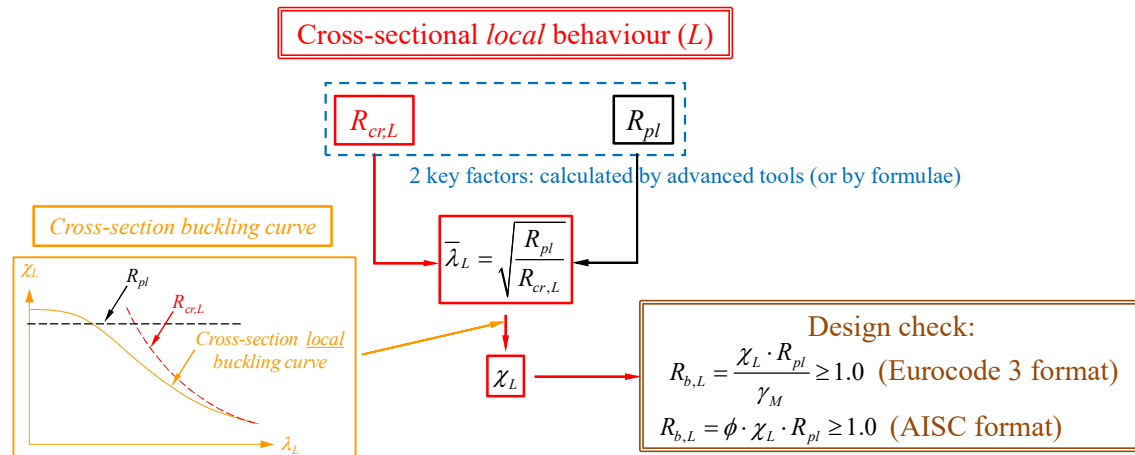
$$\text{When } \frac{N_{Ed}}{N_{c,Rd}} < 0.2 \quad \frac{N_{Ed}}{2 \cdot N_{c,Rd}} + \frac{8}{9} \cdot \left(\frac{M_{y,Ed}}{M_{c,Rd,y}} + \frac{M_{z,Ed}}{M_{c,Rd,z}} \right) \leq 1 \quad (5)$$

2.3 Alternative design philosophies

Due to the various shortcomings mentioned previously, some innovative methods for steel design were developed in recent years, such as the D.S.M. (Schafer, 2008) or the C.S.M. (Gardner, 2008). These methods present advantages in their specific scope of application. The D.S.M. is a design method primarily aimed at the design of cold-formed steel sections (Schafer, 2008), which was then extended to other materials and loading situations (Li, 2014; Torabian and Schafer, 2018). It relies on the assumption that member resistance can be calculated from the ratio of the yield stress to the elastic critical stress through specific “buckling curves”. As being originally dedicated to very slender cold-formed steel sections and based on elastic principles, the D.S.M. does not specifically address stocky sections which are a lot more influenced by plastic behaviour.

The C.S.M., instead, is a strain-based approach that is best suited to (very) compact sections. It establishes relationships between cross-sectional resistance and deformation capacity, and can get benefits from strain hardening effects when large strain levels are reachable. It was primarily derived for stocky stainless steel sections and members (Afshan and Gardner, 2013; Gardner, 2008) and then extended to compact carbon steel hot-rolled steel sections (Yun et al., 2018c) and finally broadened to slender sections (Zhao et al., 2017). Yet, the C.S.M. does not provide a direct prediction of the resistance but rather a maximum expected cross-section strain level; too, the strain-based nature of the method is not particularly suited to slender sections, for which overall strain levels are quite limited and stain hardening benefits inexistent.

Eventually, the O.I.C. emerged as a means to further address the previously-cited shortcomings: based on the well-established resistance-instability interaction through an extended definition of a generalised relative slenderness, it provides a direct, simple yet accurate determination of the ultimate resistance of steel elements. It abandons the cross-section classification concept and the E.W.M., and applies to all cross-section shapes in a similar way for both sections and members, either for simple or combined loading cases. Boissonnade et al. introduced the bases, principles and application steps of the O.I.C in (Boissonnade et al., 2017) and detailed its mechanical background. The O.I.C. has been developed for hollow steel sections on cross-section level and member level (Hayeck, 2016; Nseir, 2015), respectively. Beyer (Beyer, 2017) extended the O.I.C. approach to U-sections members subjected to combined loadings of compression axial forces, biaxial bending and torsion. Eventually, a design proposal for the local resistance of hot-rolled and welded I-sections under simple load cases was presented in (G erard et al., 2021). As a particular feature, the O.I.C. opens the door to relying on advanced tools for the calculation of key coefficients for an improved design accuracy, see Fig. 1.



3. Numerical models – Validation and parametric studies

All numerical results presented in this paper were computed through non-linear finite element analyses using software ABAQUS (Abaqus, 2011). S4R shell element with 4-nodes doubly curved and reduced integration was adopted, since it has been proved to provide excellent performance levels in former studies on sections and members resistance (Bock et al., 2015; Yuan et al., 2015). Both Linear Buckling Analyses (L.B.A.) by means of the subspace iteration method and Geometrically and Materially Non-linear with Imperfections Analyses (G.M.N.I.A.) through the so-called “Riks method” were performed. Mesh sensitivity studies for both L.B.A. and G.M.N.I.A. were conducted beforehand to guarantee a good balance between accuracy of results and computing efficiency. Section dimensions considered in the present study being quite variable, a relative mesh size of $1 / 24^{\text{th}}$ of the web dimension was finally chosen to guarantee a sufficient discretization in the models. A standardised quad-linear stress-strain relationship (Yun and Gardner, 2017) was used for both validation purposes (also paired with measured properties) and along parametric studies. For hot-rolled I-sections, the fillet zones between web and flange plates were modelled carefully by using extra beam and spring elements to simulate the real geometry in this area (Beyer, 2017; Gérard et al., 2021; Li et al., 2022b).

In the current study, the numerical models were validated against experimental data in (Greiner et al., 2009). Measured dimensions, stress-strain relationships and geometrical imperfections were all implemented in the ABAQUS models. Experimental boundary conditions, as shown in Fig. 2a, were modelled by using rigid body constraints at the end-sections to replicate very thick and nearly rigid end-plates. In the two reference points as shown in Fig. 2b, the horizontal displacements U_z , U_y as well as the rotation movement θ_x were constrained. The horizontal distance e_x between the supports and the end sections was kept as 20 mm to reproduce the test arrangement (Greiner et al., 2009). Point loads were applied with biaxial eccentricities, e_y and e_z , with respect to the centroid, to generate extra bending moments as was done in the experimental setup.

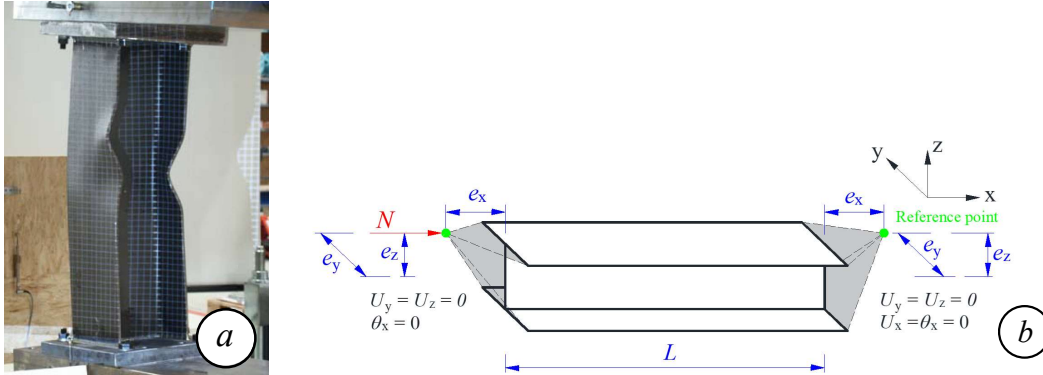


Fig. 2. a) Picture of specimen in test rig after testing – b) Boundary conditions in F.E. model.

Two distinct residual stresses patterns as suggested in (Gérard, 2019) were considered in the F.E. models for hot-rolled and welded I-sections to simulate initial stress states arising from two distinct manufacturing procedures. As shown in Fig. 3, a parabolic residual stresses pattern with a maximum stress of 235 MPa (f_y 235) is used for hot-rolled I-sections, leading to a distribution of residual stresses in self-equilibrium on a plate-per-plate basis – this makes β , β_1 and β_2 factors to be geometry-dependent.

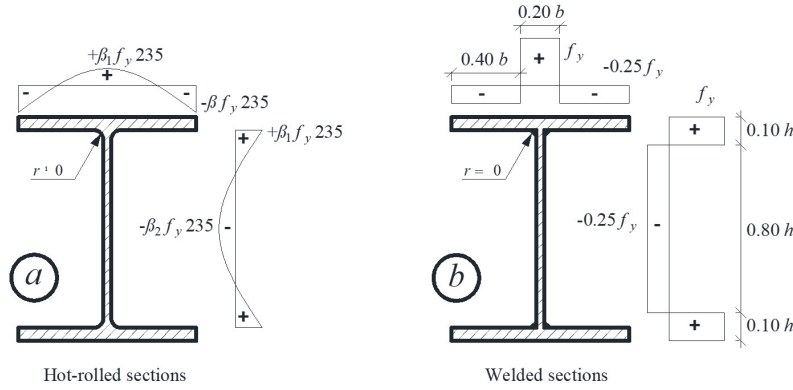


Fig. 3. Residual stresses patterns – a) In hot-rolled sections – b) In welded sections (rolled flanges).

Local geometrical imperfections were introduced in the numerical models by modifying nodes coordinates through sinusoidal functions, as has been applied in many previous studies (Gérard, 2019; Gérard et al., 2019; Gérard et al., 2021) and proved to be accurate and efficient. The maximum amplitudes of sinusoidal functions were chosen as $1 / 200^{\text{th}}$ of each individual “plate buckling length a_i ”, namely as $a_w = h - 2 t_f - 2 r$ for webs and $a_f = b - t_w - 2 r$ for flange plates. The $1 / 200$ amplitude values follow previous detailed analyses on this matter (Hayeck, 2016; Johansson et al., 2007; Kettler, 2008), and can be shown realistic yet safe, thus appropriate. Note that this $1 / 200$ amplitude considered here stems primarily from measurements and do not include the influence of residual stresses, as typical equivalent geometrical imperfections do. Also, the fillets’ radius r was set to zero for welded I-sections, as shown in Fig. 4.

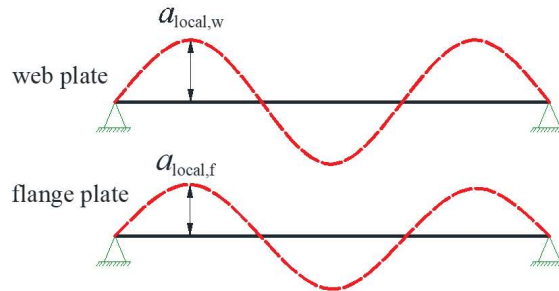


Fig. 4. Initial local geometrical imperfection shapes.

The comparison between F.E. results and experimental results is summarized in Fig. 5, where $N_{u, \text{Exp}}$ and $N_{u, \text{F.E}}$ represent the peak loads recorded during testing and computed numerically, respectively. If $N_{u, \text{F.E}} / N_{u, \text{Exp}} < 1.0$, the F.E. resistance predictions are on the safe side, while if $N_{u, \text{F.E}} / N_{u, \text{Exp}} > 1.0$, the numerical results are unsafe. A total of 22 combined loading situations were considered in the validation process. It is shown that the maximum value of $N_{u, \text{F.E}} / N_{u, \text{Exp}}$ ratio is 1.10 with a minimum $N_{u, \text{F.E}} / N_{u, \text{Exp}}$ equal to 0.95. The average value of all $N_{u, \text{F.E}} / N_{u, \text{Exp}}$ ratios is less than 1.02 with a very satisfactory Coefficient of Variation (C.O.V.) lower than 0.04. Accordingly, it is concluded that the F.E. models are reliable in predicting the ultimate resistances of I-sections under various combined load cases. More details relative to these validation studies are provided in (Li et al., 2022a; Li et al., 2022b).

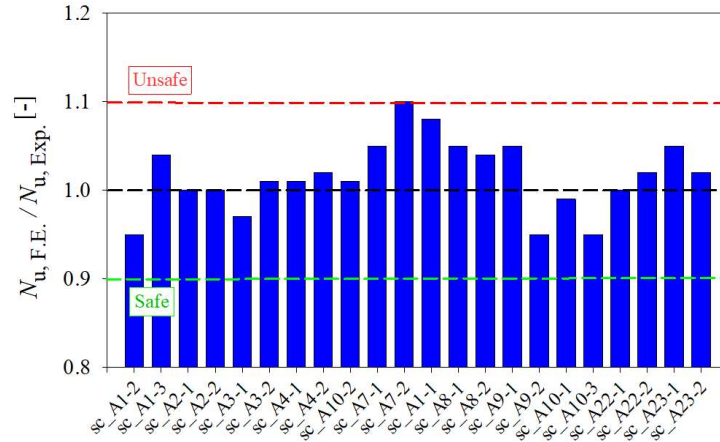


Fig. 5. Comparisons between F.E. results and experimental results.

4. Parametric studies

Based on the validated numerical models, a series of numerical computations was conducted to gather F.E. results over a broad range of steel grades, cross-section dimensions and combined load cases. The objective was to collect a large number of reference results, covering the whole spectrum of combined loading situations, in order to assess the accuracy of the interaction equations suggested in (AISC, 2010; EN 1993-1-1, 2005), as well as O.I.C.-based design proposals.

Nominal section dimensions and material properties were adopted in the F.E. models along these parametric studies. Rigid body boundary conditions were adopted again in order to fix warping at the end sections, and therefore enable a potential complete yielding of the section (Kindmann and Wolf, 2004; Li et al., 2022a; Li et al., 2022b; Rubin, 1978). The combined loadings were simulated by applying concentric compression and bending moments directly at two reference points which are located in the centroid of end-sections. To ensure that the members are long enough to limit the influence of support conditions but short enough to avoid any significant effect of member instability, i.e., lateral torsional buckling and/or flexural torsional buckling. The Lengths L were set as three half-wavelengths of the flange plate buckling length in accordance with previous studies (Li et al., 2022a).

Various parameters have been considered, as follows:

- 3 steel grades: 2 “standard” ones, S355 ($f_y = 355$ MPa) and S460 ($f_y = 460$ MPa), and one high strength steel grade S690 ($f_y = 690$ MPa) – note that S690 steel for hot-rolled sections was here only accounted for in order to extend the application scope of the present study;
- Two manufacturing processes resulting in 2 “families” of I-sections: hot-rolled and welded, and among them:
 - 140 different geometries of *hot-rolled* I-sections, chosen from European and American usual catalogues (ArcelorMittal Europe, 2019; *Handbook of Structural Steelwork: Eurocode edition*, 2013; *Steel Construction Manual*, 2017). Height h varied from 100 to 1108 mm, width b from 55 to 424 mm, web thickness t_w from 4.1 to 45.5 mm, and flange thickness t_f from 5.2 to 82 mm. Therefore, section aspect ratio h / b ranges from 1.0 to 3.4, and section classes vary from compact to slender (i.e., Class 1 to Class 4). These hot-rolled geometries involve non-slender flanges but slightly to more slender webs: the

web plate slenderness h/t_w ranges from 19.9 to 63.0 and flange plate slenderness $b/(2t_f)$ varies from 2.5 to 10.8;

- 106 geometries of *welded* I-sections, from regular ones available in usual catalogues (*Handbook of Structural Steelwork: Eurocode edition*, 2013; *Handbook of steel construction*, 2017; *Steel Construction Manual*, 2017) including Class 1 to Class 4 sections, and some additional invented sections obtained with reductions in the thickness of webs and flanges aiming at obtaining more slender sections (i.e., more sensitive to local buckling), in an effort to widen the range of applicability of the present research. The height h varied from 80 to 1008 mm, width b from 46 to 1000 mm, web thickness t_w from 3.8 to 21.0 mm, and flange thickness t_f from 5.2 to 40 mm. Obviously, section dimensions were carefully selected and associated so as to lead to suitable properties: h/b ratios ranges from 0.7 to 3.3, h/t_w from 12.3 to 128.4 and $b/(2t_f)$ from 3.3 to 26.3. Overall, flanges vary from semi-compact to slender, whereas webs span from slightly to very slender.
- 10 combined load cases as listed in Table 2, which includes two $N+M_y$ cases, two $N+M_z$ cases, two M_y+M_z cases and four $N+M_y+M_z$ cases. Each subcase is defined according to the 3-dimension load surface illustrated in Fig. 6, where n , m_y and m_z respectively represent the axial, major-axis and minor-axis bending applied forces relative to their respective plastic capacities. This surface can be characterized through spherical coordinates where each point can be defined through three parameters, i.e., polar angle θ , azimuthal angle φ and radial distance $\chi_{L,combined}$, see Eqs. (6) and (7). The selection of θ and φ angles in Table 2, which vary from 0° to 90° , allows to completely cover the range of compression and bi-axial bending cases, from low to dominant compression, with bending being either predominantly about the major-axis or about the minor-axis, as well as all intermediate configurations. Each simple load case, i.e., N , M_y or M_z , is therefore represented by specific 0° or 90° θ and φ angles, while more complex combinations are associated to intermediate angle values. Angles θ and φ characterize the relative influence of compression (θ , see Eq. (6)) and the balance between M_y and M_z bending moments (φ , see Eq. (7)). With a decrease in angle θ , the compression force governs, whereas a decrease in φ leads to a dominant major-axis bending moment. Accordingly, any given load combination that is such that the resulting point in the $n-m_y-m_z$ space lies inside or on the resistance surface means that the carrying capacity check is fulfilled, while any point outside the surface indicates an unsafe design. In accordance with the previous sets of parameters, each load case comprised 420 F.E. simulations for hot-rolled sections and 318 ones for welded sections.

Table 2. Combined load cases considered and associated dominant forces.

Load case	Polar angle θ	Azimuthal angle φ	Dominant force
$N+M_y$	$\theta = 30^\circ$	$\varphi = 0^\circ$	N
	$\theta = 60^\circ$		M_y
$N+M_z$	$\theta = 30^\circ$	$\varphi = 90^\circ$	N
	$\theta = 60^\circ$		M_z
M_y+M_z	$\theta = 90^\circ$	$\varphi = 30^\circ$	M_y
		$\varphi = 60^\circ$	M_z
$N+M_y+M_z$	$\theta = 30^\circ$	$\varphi = 30^\circ$	N and M_y
		$\varphi = 60^\circ$	N and M_z
	$\theta = 60^\circ$	$\varphi = 30^\circ$	M_y
		$\varphi = 60^\circ$	M_z

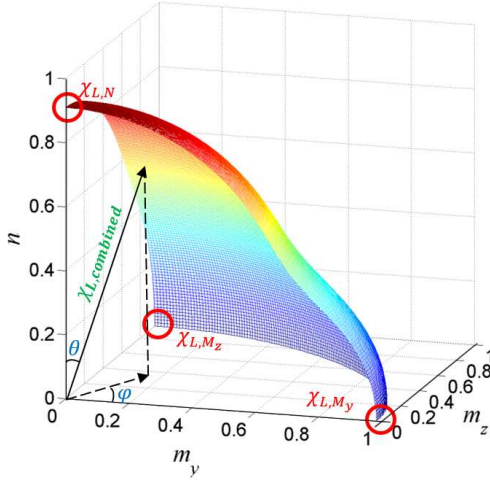


Fig. 6. 3-dimensional n - m_y - m_z loading space.

$$\tan \theta = \frac{m_y}{n \cdot \cos \varphi} = \frac{m_z}{n \cdot \sin \varphi} \quad (6)$$

$$\tan \varphi = m_z / m_y \quad (7)$$

An early set of results aiming at comparing the influence of different yield stresses is illustrated in Fig. 7 in a so-called “O.I.C. format”, where the horizontal axis represents the generalized slenderness λ_L (see definition in Fig. 1) that takes the balance between plastic resistance and stability, while the vertical axis χ_L refers to a so-called “penalty (or reduction) factor” that aims at accounting for the detrimental influence that buckling and imperfections have on plastic capacity kept as a reference. This format simply consists in an extension of the Ayrton-Perry format (Ayrton and Perry, 1886; Maquoi and Rondal, 1978) classically used for member resistance. Also, in Fig. 7 and many following ones, two reference curves are also included besides the F.E. results: the horizontal solid line represents plastic resistance, i.e., $\chi_L = 1.0$, while a hyperbolic dashed line plots the Von Karman’s elastic plate buckling curve for the design of ideal plates without imperfections, i.e., $\chi_L = 1 / \lambda_L$.

Thanks to the O.I.C. general format, results for all steel grades can be presented on a single figure, and Fig. 7a plots all results obtained for hot-rolled sections, while Fig. 7b is dedicated to welded sections.

Figs. 7a and 7b first illustrate that large amounts of F.E. results were obtained, spanning a wide range of slenderness – from compact Class 1 to Class 4 (very) slender sections. Comparison of Fig. 7a with Fig. 7b shows that quite different results are obtained between the two fabrication processes, namely with respect to the large scatter observed for welded sections in Fig. 7b, as a consequence of (i) more detrimental residual stresses and (ii) quite more slender section parts.

The figures also show the relatively low influence of the steel grade on the results, confirming that the influence of the material grade is sufficiently accounted for within the O.I.C. format. Yet, considering a single, safe-sided curve in each case (hot-rolled and welded I-sections) would appear quite over-conservative and uneconomical. In this respect, detailed analyses of all results have shown that key parameters associated to the scatters observed on Figs 7a and 7b shall be of geometrical nature (see also (Gérard et al., 2021)). In particular, the influences of the following ratios have shown important:

- the ratio of plates’ widths h / b ;
- the ratio between plates’ areas $(h \cdot t_w) / (b \cdot t_f)$;

- the plates' respective slenderness h / t_w and b / t_f .

Several combinations of these parameters were studied to select a unique yet simple leading parameter. It shall be noted here that (i) the use of a single parameter yields a strong constraint towards accurate resistance predictions and that (ii) not only simple and combined load cases of doubly-symmetric I-sections but also mono-symmetric I-sections were considered for the selection of the final γ_{HR} and γ_W parameters suggested hereafter; more details are given in Section 5 and in (Gérard et al., 2021; Li et al., 2022a; Li and Boissonnade, 2023).

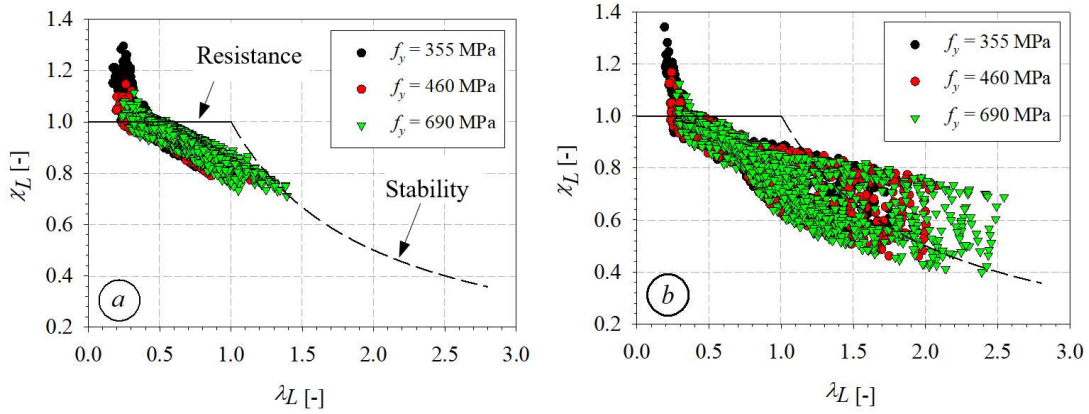


Fig. 7. Influence of different steel grades – a) Hot-rolled sections – b) Welded sections.

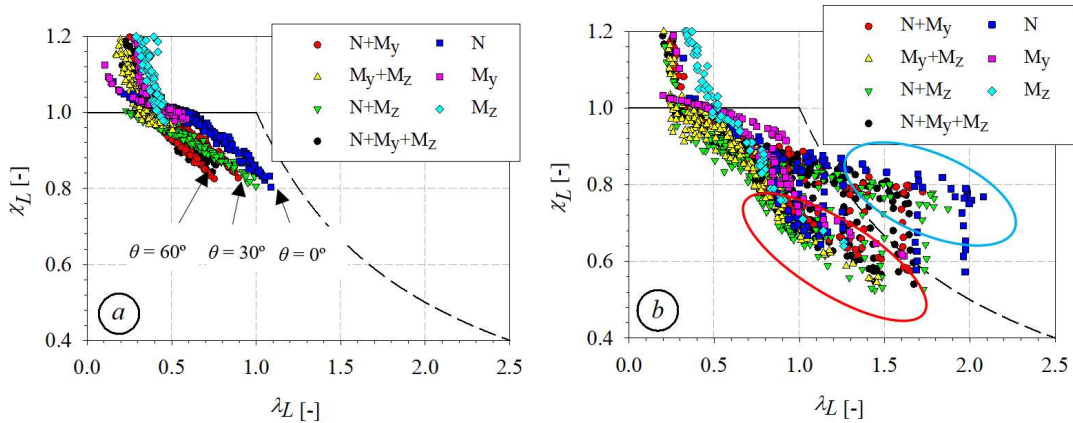


Fig. 8. F.E. results for different combined loading situations – a) Hot-rolled sections – b) Welded sections.

Table 3. Distribution of section classification for different load cases.

	Hot-rolled sections			Welded sections		
	Class 1-2	Class 3	Class 4	Class 1-2	Class 3	Class 4
Case 1	$N+M_y (\theta = 30^\circ, \varphi = 0^\circ)$					
Whole section	16.1%	40.8%	43.1%	6.0%	15.4%	78.6%
Web	21.3%	37.4%	41.3%	6.6%	17.9%	75.5%
Flange	82.3%	16.0%	1.7%	36.4%	20.8%	42.8%
Case 2	$N+M_y (\theta = 60^\circ, \varphi = 0^\circ)$					
Whole section	16.4%	69.5%	14.1%	6.0%	28.9%	65.1%
Web	21.4%	66.2%	12.4%	6.6%	39.3%	54.1%
Flange	82.0%	16.2%	1.8%	36.4%	20.8%	42.8%
Case 3	$N+M_z (\theta = 30^\circ, \varphi = 90^\circ)$					
Whole section	17.5%	13.1%	69.7%	6.0%	2.8%	91.2%
Web	22.2%	8.1%	69.7%	6.6%	2.2%	91.2%
Flange	82.4%	17.0%	0.6%	36.5%	23.9%	39.6%
Case 4	$N+M_z (\theta = 60^\circ, \varphi = 90^\circ)$					
Whole section	17.2%	13.1%	69.7%	6.1%	2.9%	91.0%
Web	22.2%	8.1%	69.7%	6.7%	2.3%	91.0%
Flange	82.3%	17.3%	0.3%	36.0%	25.1%	38.9%

Fig. 8 proposes a first view of results for S355 steel grade, involving many different load combinations, and classified per combined load cases. For better comparison, a summary is made for $N+M_y$ and $N+M_z$ cases in Table 3 where the distribution of section classes is based on Eurocode 3. Both Fig. 8 and Table 3 allow for a first set of observations, and indicate that:

- The O.I.C. format allows all combined loading cases to be expressed in a similar way (i.e., $\chi_L - \lambda_L$ format) and keep them with a satisfactory continuity. Also, as expected, the combined loading cases are seen to behave as extensions from the three simple N , M_y and M_z load cases;
- Residual stresses patterns of welded sections are more detrimental than hot-rolled ones (see Fig. 3). Therefore, for a given section shape, welded sections usually achieve lower resistances;
- For hot-rolled sections whose section dimensions were determined from standardized catalogues, Table 3 reports that more than 80% of flange plates belongs to Class 1-2, regardless of the whole sections class, while more than 70% of webs belong to Class 3 or 4 for $N+M_y$ and $N+M_z$ cases; reason is that most of the hot-rolled sections are meant to be used as beams, thus the relatively stocky flanges but the more slender web plates. Therefore, in most of the combined loading cases reported on Figs. 8a and 8b, the loss in section strength shall mostly be attributed to web local buckling under non-uniform compression stresses. That is also the reason why for the the M_y+M_z cases, in which local buckling mostly occurs in flanges, the section slenderness λ_L of hot-rolled sections can roughly reach 0.5, whereas λ_L for welded sections can reach up to 1.5;
- As illustrated in Table 3, the web plates (and also sections) become stockier when they are subjected to a lower level of axial compression, e.g., for $N+M_y$ cases; therefore, as shown in Fig. 8a, some results appear to be “shifted” from the simple compression N case to combined $N+M_y$ cases with $\theta = 30^\circ$ and then to the $N+M_y$ cases with $\theta = 60^\circ$;
- For $N+M_z$ cases, the plate or section slenderness do not change significantly, so that no evident trends are observable in the results;

- Welded sections typically exhibit more scattered patterns than hot-rolled sections:
 - Firstly, their dimensions have been chosen to vary in greater extents than hot-rolled sections. In particular, more slender sections were studied, and their slenderness λ_L can reach up to 2.0, while the maximum λ_L of hot-rolled is around 1.2;
 - Secondly, Table 3 reports that more than 60% of flanges belong to Class 3 or 4, so the sections may fail by web-flange interactive local buckling. The latter can be shown especially relevant for the results with lowest section resistances as highlighted in the red ellipse of Fig. 8b, where both the web and flanges belong to Class 3 or 4;
 - Last, some of the “invented” slender welded I-sections show significant post buckling effects as shown by the blue ellipse on Fig 8b, so their resistance could reach higher levels;
- For both hot-rolled and welded sections, the slenderness λ_L of a section under combined loading is usually within the range of its corresponding simple loading cases λ_L 's. However, its penalty factor χ_L is sometimes observed to be lower than the resistance of its corresponding simple loading cases values, i.e., χ_N , χ_{M_y} or χ_{M_z} . Accordingly, in a 3-dimensional N - M_y - M_z loading space (see Fig. 8), the resistance surface cannot be represented by a simple shape, such as a perfect spherical or ellipsoidal one, in which resistance χ_L is within the range of χ_N , χ_{M_y} and χ_{M_z} . Depending on sections' behaviour at their ultimate state, the true resistance surface can be relatively less convex than a perfect spherical or ellipsoidal surface. In particular, cases of welded sections under $N+M_z$ seem to be the most detrimental ones since section resistances are 6% to 26% lower than the average of their corresponding χ_N and χ_{M_z} counterparts. In this respect, all such phenomena should be properly considered in deriving a new accurate design approach for I-shapes under combined loading situations, as described in the next paragraphs.

5. Proposed design rules

5.1 O.I.C. approach

The extended O.I.C. format is defined as in Eqs. (8) and (9), where λ_0 characterizes the length of a $\chi_L = 1.0$ plateau, α_L considers the influence of imperfections and δ accounts for any post-buckling effects. Factor β captures possible strain hardening effects which may lead to a carrying capacity of the section slightly higher than the plastic resistance, i.e., χ_L could be larger than unity when $\beta > 1$. Although $\chi_L > 1.0$ results may be observed for the most compact sections at the local level, the benefits of strain hardening for carbon steel is known to vanish at the member level – see for example the study of Hayeck (Hayeck, 2016). Accordingly, in this paper, the value of β is deliberately kept as 1.0; this condition influences the accuracy of the proposed O.I.C. approach for the most compact sections, as we shall see in the following paragraphs.

$$\chi_L = \frac{\beta}{\phi_L + \sqrt{\phi_L^2 - \lambda_L^\delta \cdot \beta}} \quad (8)$$

$$\text{Where } \phi_L = 0.5 \cdot (1 + \alpha_L \cdot (\lambda_L - \lambda_0) + \lambda_L^\delta \cdot \beta) \quad (9)$$

All these factors were calibrated according to numerical reference results. The present paper being an extension of the study on I-shapes under simple loading, for which O.I.C. expressions have been proposed in (Gérard et al., 2021) and proved to be more precise and consistent than current steel design proposals, similarities in O.I.C. design equations for combined loading

situations are to be expected. In particular, identical γ_{HR} and γ_W factors have been adopted – see also Table 4, which recalls O.I.C. design factors for simple load cases.

Table 4. O.I.C design factors for simple load cases.

	Hot-rolled I-sections	Welded I-sections
Key parameters	$\gamma_{HR} = \frac{b}{t_f} \cdot \left(\frac{h}{t_w} \right)^2 \cdot \frac{t_w}{t_f} \cdot 10^{-5}$	$\gamma_W = \frac{b}{h} \cdot \frac{t_w}{t_f}$
Compression (N)	$\lambda_0 = 0.45$ $\alpha_L = 0.1 \cdot \gamma_{HR} + 0.005$ $\delta = 0.01/\gamma_{HR} + 0.31$	$\lambda_0 = 0.5$ $\alpha_L = 0.43 \cdot \gamma_W - 0.034$ $\delta = 0.32 \cdot \gamma_W + 0.23$
Major-axis bending (M_y)	$\lambda_0 = 0.4$ $\alpha_L = -0.3 \cdot \gamma_{HR}^2 + 0.26 \cdot \gamma_{HR} + 0.02$ $\delta = -3.64 \cdot \gamma_{HR}^2 + 2.11$	$\lambda_0 = 0.5$ $\alpha_L = 1.15\sqrt{\gamma_W} - 0.84 \cdot \gamma_W - 0.26$ $\delta = 0.4$
Minor-axis bending (M_z)	$\lambda_0 = 0.35$ $\alpha_L = 0.08$ $\delta = 1.54$	$\lambda_0 = 0.35$ $\alpha_L = 0.08$ $\delta = 1.54$

5.2 O.I.C. approach for combined loading situations

An O.I.C.-based approach for the design of cross-sections under combined load cases has been developed using the three-dimensional n - m_y - m_z loading space and the 3D resistance surface of Fig. 6. Further to the three end points, the general and local shape of the resistance surface is also a key factor affecting the accuracy of resistance predictions for combined loading situations. Therefore, in order to ensure an optimal accuracy of resistance predictions, the design surfaces shall be as close as possible to the F.E.-generated resistance ones. In this respect, an interaction equation for mono-symmetric I-sections under combined loading is proposed here and defined by Eq. (10), which simply originates from the spherical coordinates system illustrated in Fig. 6. The six q_i parameters in Eq. (10) can (i) suitably adjust the curvature of the design surface and (ii) ensure continuity between simple and combined load cases. More precisely, the q_1 parameter, which appears at several places, guarantees the resistance reduction coefficient $\chi_{L,combined}$ to converge to the simple loading limit states, i.e., to $\chi_{L,N}$, χ_{L,M_y} and χ_{L,M_z} , as well as allows modifying the *general shape* of the design surface. In contrast, q_2 to q_6 factors only have an impact on *certain parts* of the surface and allows to “locally” adjust its shape. Based on local calibration with the numerical results collected in Section 4, the proposed q_i parameters, summarised in Table 5, have been adjusted to be applicable for I-sections under various combined load cases. More background information about the interaction design equation Eq. (10) and its q_i parameters can be found in (Li et al., 2022a).

$$\chi_{L,combined} = \left[\left(\chi_{L,N} \cdot \cos^{q_2} \theta \right)^{q_1} + \left(\chi_{L,M_y} \cdot \sin^{q_3} \theta \cdot \cos^{q_4} \varphi \right)^{q_1} + \left(\chi_{L,M_z} \cdot \sin^{q_5} \theta \cdot \sin^{q_6} \varphi \right)^{q_1} \right]^{\frac{1}{q_1}} \quad (10)$$

Table 5. O.I.C. design factors for combined load cases.

q factors	q_1	q_2	q_3	q_4	q_5	q_6
Hot-rolled sections	8	0.2	2	0.3	1	0.4
Welded sections	8	0.3	1	0.6	2	0.6

6. Performance assessment of the O.I.C. proposal and comparison to existing codes

6.1 Design proposal for hot-rolled sections

Figs. 9 and 10 present overall and summary results on the comparison between the O.I.C. proposal and the numerical results, as well as equivalent results for Eurocode 3 and the American Standards design rules, for $N+M_y$ cases ($\theta = 30^\circ$, $\varphi = 0^\circ$) and $N+M_y+M_z$ cases ($\theta = 30^\circ$, $\varphi = 30^\circ$) – it is reminded that $\theta = 30^\circ$ is associated to a high level of relative compression and that $\varphi = 0^\circ$ indicates no participation of minor-axis bending, while $\varphi = 30^\circ$ for the $N+M_y+M_z$ cases means that although minor-axis bending is non zero, major-axis bending is dominant.

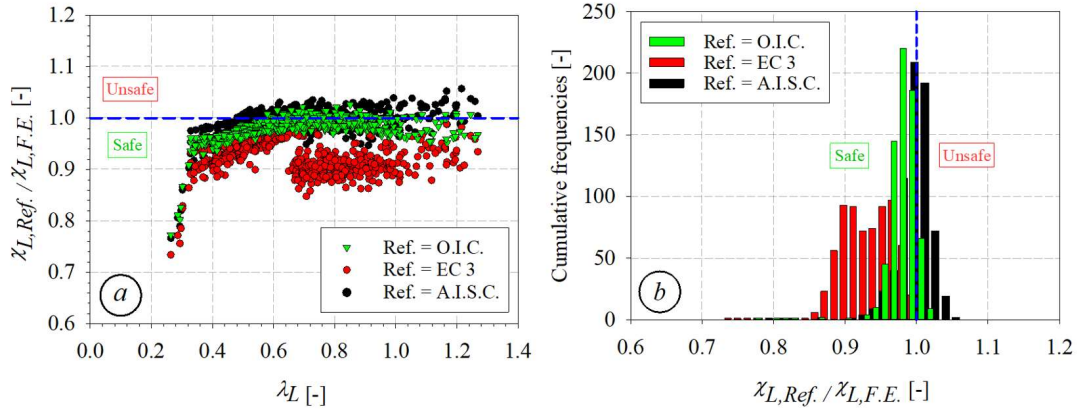


Fig. 9. Analytical predictions vs. F.E. reference results for hot-rolled sections – $N+M_y$ ($\theta = 30^\circ$, $\varphi = 0^\circ$).

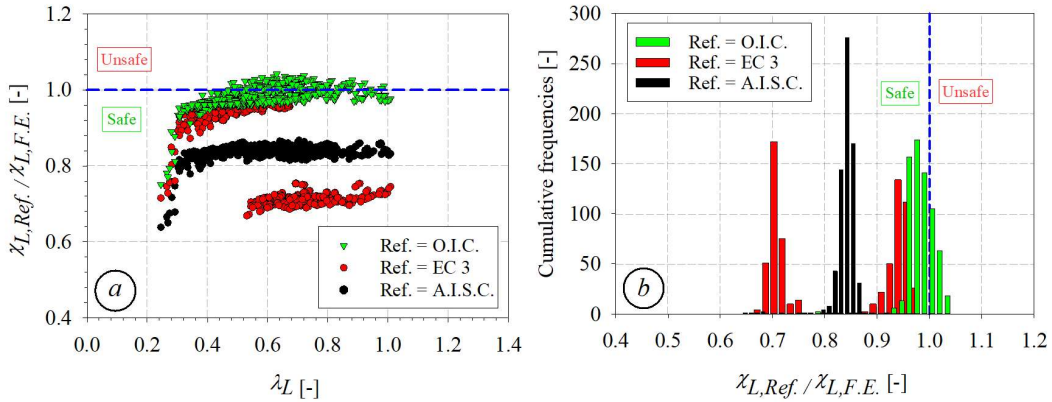


Fig. 10. Analytical predictions vs. F.E. reference results for hot-rolled sections – $N+M_y+M_z$ ($\theta = 30^\circ$, $\varphi = 30^\circ$).

Figs. 9a and 10a plot the ratio $\chi_{L,Ref.} / \chi_{L,F.E.}$ for any of the design proposals' resistances to the F.E. reference results as a function of the sections' slenderness λ_L , while Figs. 9b and 10b show the cumulative frequencies of the $\chi_{L,Ref.} / \chi_{L,F.E.}$ ratios. $\chi_{L,Ref.}$ represents the resistance predicted by either Eurocode 3 rules, the American Standards equations or the O.I.C. proposal, and $\chi_{L,F.E.}$ designates the F.E. results, kept as a reference. When $\chi_{L,Ref.} / \chi_{L,F.E.}$ is less than one, the analytical prediction of the resistance is on the safe side, but when $\chi_{L,Ref.} / \chi_{L,F.E.}$ is larger than one, the prediction is on the unsafe side. Various complementary statistical data relative to $\chi_{L,Ref.} / \chi_{L,F.E.}$ ratios are shown in Table 6, such as the mean value, the C.O.V., the maximum ratio value, the minimum value, and the percentage of resistance predictions over 3% and 10% on the unsafe

side. The latter 3% and 10% indicators have been chosen to point out, respectively, the amount of slightly unsafe predictions or more seriously unsafe results for which usual partial safety factors may not compensate for inaccuracies associated to the design model itself.

Table 6. Statistical results of $\chi_{L,Ref.} / \chi_{L,F.E}$ ratio for all hot-rolled sections.

Load cases	Proposals	Mean	C.O.V.	Max.	Min.	> 1.03	> 1.10
All load cases	O.I.C.	0.971	0.039	1.065	0.702	2.3%	0.0%
	EC 3	0.836	0.179	1.049	0.472	0.0%	0.0%
	A.I.S.C.	0.821	0.123	1.070	0.592	1.2%	0.0%
$N+M_y$ ($\theta = 30^\circ, \varphi = 0^\circ$)	O.I.C.	0.981	0.022	1.026	0.773	0.0%	0.0%
	EC 3	0.934	0.038	1.004	0.734	0.0%	0.0%
	A.I.S.C.	0.992	0.027	1.057	0.766	2.3%	0.0%
$N+M_y$ ($\theta = 60^\circ, \varphi = 0^\circ$)	O.I.C.	0.938	0.037	0.993	0.702	0.0%	0.0%
	EC 3	0.931	0.048	1.049	0.688	0.4%	0.0%
	A.I.S.C.	0.996	0.037	1.070	0.741	9.2%	0.0%
$N+M_z$ ($\theta = 30^\circ, \varphi = 90^\circ$)	O.I.C.	1.006	0.023	1.065	0.948	15.7%	0.0%
	EC 3	0.769	0.160	0.977	0.654	0.0%	0.0%
	A.I.S.C.	0.854	0.017	0.882	0.803	0.0%	0.0%
$N+M_z$ ($\theta = 60^\circ, \varphi = 90^\circ$)	O.I.C.	0.979	0.022	1.036	0.885	0.9%	0.0%
	EC 3	0.662	0.253	0.951	0.521	0.0%	0.0%
	A.I.S.C.	0.794	0.020	0.825	0.734	0.0%	0.0%
M_y+M_z ($\theta = 90^\circ, \varphi = 30^\circ$)	O.I.C.	0.975	0.031	1.032	0.810	0.1%	0.0%
	EC 3	0.946	0.036	0.993	0.698	0.0%	0.0%
	A.I.S.C.	0.800	0.033	0.858	0.662	0.0%	0.0%
M_y+M_z ($\theta = 90^\circ, \varphi = 60^\circ$)	O.I.C.	0.984	0.030	1.056	0.841	2.7%	0.0%
	EC 3	0.925	0.040	0.980	0.596	0.0%	0.0%
	A.I.S.C.	0.743	0.032	0.785	0.642	0.0%	0.0%
$N+M_y+M_z$ ($\theta = 30^\circ, \varphi = 30^\circ$)	O.I.C.	0.983	0.029	1.042	0.751	1.5%	0.0%
	EC 3	0.835	0.142	0.985	0.669	0.0%	0.0%
	A.I.S.C.	0.836	0.024	0.868	0.638	0.0%	0.0%
$N+M_y+M_z$ ($\theta = 30^\circ, \varphi = 60^\circ$)	O.I.C.	0.999	0.023	1.040	0.844	2.2%	0.0%
	EC 3	0.751	0.210	0.970	0.571	0.0%	0.0%
	A.I.S.C.	0.754	0.021	0.786	0.617	0.0%	0.0%
$N+M_y+M_z$ ($\theta = 60^\circ, \varphi = 30^\circ$)	O.I.C.	0.920	0.036	0.971	0.749	0.0%	0.0%
	EC 3	0.832	0.136	0.954	0.557	0.0%	0.0%
	A.I.S.C.	0.743	0.031	0.785	0.592	0.0%	0.0%
$N+M_y+M_z$ ($\theta = 60^\circ, \varphi = 60^\circ$)	O.I.C.	0.940	0.020	0.967	0.830	0.0%	0.0%
	EC 3	0.784	0.249	0.955	0.472	0.0%	0.0%
	A.I.S.C.	0.689	0.023	0.724	0.610	0.0%	0.0%

As shown in Fig. 9 and Table 6, all three proposals perform relatively well for $N+M_y$ cases with dominant N ($\theta = 30^\circ$) and M_y ($\varphi = 0^\circ$), since the mean values of $\chi_{L,Ref.} / \chi_{L,F.E}$ reported for all design approaches remain over 0.93, C.O.V. values are less than 0.04 and the “worse” result is within 6% of the unsafe side. Yet, the Eurocode is seen less accurate than the other two proposals, mainly because:

- A detrimental discontinuity in the prediction of resistance between Class 3 and Class 4 sections remains present for λ_L around 0.6 to 0.8. Although the latest version of Eurocode 3 addresses the discontinuity between Class 2 to Class 3 sections for simple loading cases by using an elastic-plastic section modulus W_{ep} , it still applies two different equations for Class 1-3 sections and Class 4 sections, as defined by Eqs. (1)

- and (3);
- Similarly, especially for Class 4 sections, the interaction loading surface is a plane surface fully defined by the 3 end points for simple loading cases based on elastic design and on the E.W.M., which causes the results to be more conservative than the other two methods. When it comes to $N+M_y+M_z$ cases, as shown in Fig. 9b and detailed in Table 6, resistances predicted by Eurocode 3 and the American Standards for Class 4 sections become much more conservative, and mean values of $\chi_{L,Ref.} / \chi_{L,F.E.}$ ratios wrap around 0.8;
 - Likewise, Eurocode 3 fully restricts any plastic distribution within Class 4 sections under $N+M_y+M_z$. Consequently, many hot-rolled sections belong to Class 4 under compression but are Class 1 or 2 under minor-axis bending thanks to stocky flange plates. However, the section is still classified as Class 4 under $N+M_y+M_z$. The 3 key points of the resistance surface, i.e., n , m_y and m_z , have to be calculated based on elastic properties according to Eurocode 3, which creates another discontinuity in the prediction of resistance between simple load cases and combined load cases;
 - Also, when calculating the effective properties based on the E.W.M., Eurocode 3 assumes quite pessimistic conditions, in which the effective area A_{eff} is obtained under the assumption that the whole section is entirely under compression, $W_{eff,y}$ is obtained with 100% major-axis bending and so is $W_{eff,z}$, which can be quite far from the real stress distribution at peak load, and thus unduly penalizing the design;
 - Finally, since the classification system and Class limits were mainly derived for simple load cases and some $N+M_y$ cases, the concept of classification obviously becomes less appropriate and relevant when it comes to $N+M_y+M_z$ cases (Chen et al., 2013).

Overall, the American Specifications provide better continuity performances as its design equations as defined by Eqs. (4) and (5) result in a slightly convex surface based on two interaction planes within the 3-D load space. As shown in Fig. 10b and Table 6, results for $N+M_y$ cases report mean values of 0.99 and C.O.V. of 0.03, which is better than for Eurocode 3 design rules. Yet, when it comes to $N+M_y+M_z$ cases, predictions are seen overconservative, especially for compact sections. This is to be mostly attributed to the interaction surface being convex in two dimensions but not three-dimensional. In other words, with a fixed relative compression n value, the projection of its interaction surface in the m_y-m_z plane is a straight line, but not a curved line as for example recommended by Eq. (1) in Eurocode 3.

In contrast, the O.I.C. not only provides complete continuity from simple to combined load cases but also keeps continuous resistance estimates from stocky to slender sections. As noticed from Table 6, the O.I.C. never exhibits more than 7% average discrepancy with respect to all of the F.E. results, as well as keeps the C.O.V. of the $\chi_{L,Ref.} / \chi_{L,F.E.}$ ratio to less than 4%, which is 20% to 30% lower than the other two code proposals. Although I-sections are mainly designed for $N+M_y$ and $N+M_y+M_z$ cases with low levels of minor-axis bending, the O.I.C. proposal also shows an excellent performance for the M_y+M_z cases with a mean value larger than 0.97 and a C.O.V. lower than 3.2%, while Eurocode 3 and the American Specifications behave too conservatively when a more significant participation of M_z is involved. Although some results are left in over 3% on the unsafe side, these slightly unsafe predictions can be compensated by usual values of partial safety factors, typically bringing an extra 5% to 10%

safety. Furthermore, it shall be recalled that the O.I.C. abandons both the classification system and the E.W.M., leading to a design process vastly simpler and more efficient. Overall, the O.I.C. exhibits significantly improved reliability and accuracy while maintaining design simplicity for hot-rolled sections under combined load cases.

6.2 Design proposal for welded sections

Figs. 11 and 12, relative to the behaviour and resistance of welded sections, show comparisons between the different design proposals considered herein for the cases of $N+M_y$ ($\theta = 60^\circ, \varphi = 0^\circ$) and $N+M_y+M_z$ ($\theta = 60^\circ, \varphi = 30^\circ$). Further results and detailed statistical values of all cases investigated for welded sections are summarized in Table 7.

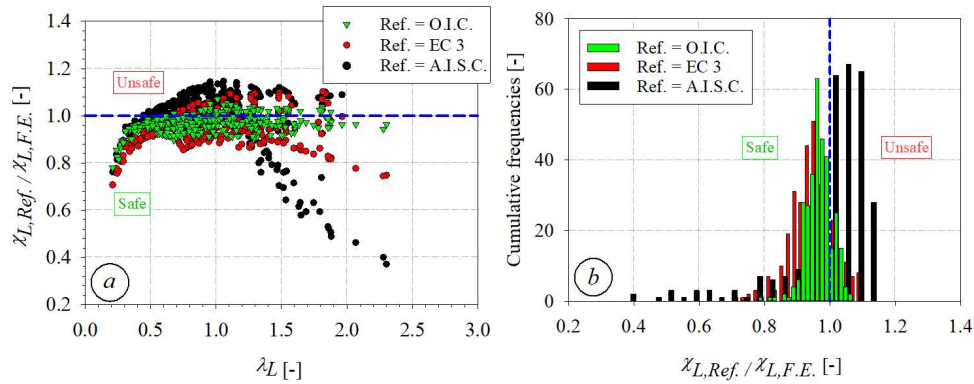


Fig. 11. Analytical predictions vs. F.E. reference results for welded sections – $N+M_y$ ($\theta = 60^\circ, \varphi = 0^\circ$).

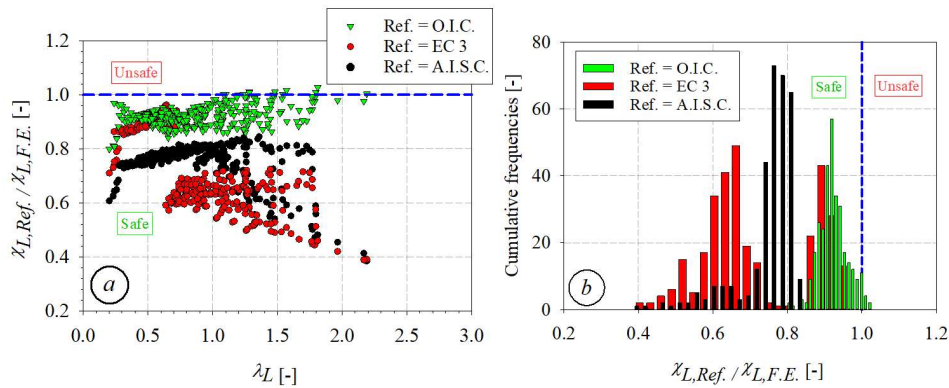


Fig. 12. Analytical predictions vs. F.E. reference results for welded sections – $N+M_y+M_z$ ($\theta = 60^\circ, \varphi = 30^\circ$).

It can be observed that the results of both Eurocode 3 and the American Specifications exhibit significant dispersions, especially for slender welded sections. For all cases, the C.O.V. of the $\chi_{L,EC3} / \chi_{L,F.E.}$ ratio is larger than 0.22 and the C.O.V. of the $\chi_{L,A.I.S.C.} / \chi_{L,F.E.}$ ratio is around 0.15, which are quite high values. Besides, for the cases of $N+M_y+M_z$, both codes seem to behave more conservatively when bending is dominant, i.e., with increases in θ and/or φ .

As shown in Fig. 11a, when λ_L is larger than 0.5, Eurocode 3 and the American Specifications exhibit more unconservative resistance predictions than hot-rolled sections, especially for “invented sections”. Detailed analysis of the results reveals that this is associated to a lack of consideration of the impact of more detrimental residual stresses arising from the manufacturing process. Especially for the American Specifications, which exhibit the worse unsafe $\chi_{L,A.I.S.C.} / \chi_{L,F.E.}$ ratio of 1.15, more than 2% of the results are still left in over 10% on the unsafe side for $N+M_y$ cases ($\theta = 60^\circ, \varphi = 0^\circ$). Besides, many sections’ resistances are

predicted over-conservatively by the American Specifications and this conservatism becomes more important with an increase in relative bending level, as seen from $N+M_y$ ($\theta = 30^\circ$, $\varphi = 0^\circ$) to $N+M_y$ ($\theta = 60^\circ$, $\varphi = 0^\circ$) cases, for which the minimum value of $\chi_{L,A.I.S.C.} / \chi_{L,F.E.}$ drops from 0.46 to 0.37 – which means that the actual strength prediction can be more than doubled. It appears that inaccurate predictions of flange buckling capacities may be the source of such over-conservatism.

Table 7. Statistical results of $\chi_{L,Ref.} / \chi_{L,F.E.}$ ratio for all welded sections.

Load cases	Proposals	Mean	C.O.V.	Max.	Min.	> 1.03	> 1.10
All load cases	O.I.C.	0.959	0.070	1.200	0.745	13.3%	2.2%
	EC 3	0.778	0.224	1.106	0.290	2.6%	0.2%
	A.I.S.C.	0.846	0.145	1.187	0.371	9.7%	2.2%
$N+M_y$ ($\theta = 30^\circ$, $\varphi = 0^\circ$)	O.I.C.	0.969	0.042	1.061	0.808	5.3%	0.0%
	EC 3	0.962	0.066	1.106	0.747	14.5%	1.3%
	A.I.S.C.	0.997	0.106	1.133	0.464	41.8%	6.6%
$N+M_y$ ($\theta = 60^\circ$, $\varphi = 0^\circ$)	O.I.C.	0.966	0.041	1.070	0.780	5.0%	0.0%
	EC 3	0.947	0.070	1.103	0.708	9.7%	0.3%
	A.I.S.C.	0.998	0.131	1.146	0.371	50.3%	13.2%
$N+M_z$ ($\theta = 30^\circ$, $\varphi = 90^\circ$)	O.I.C.	1.023	0.055	1.194	0.861	41.5%	10.7%
	EC 3	0.753	0.127	1.020	0.426	0.0%	0.0%
	A.I.S.C.	0.913	0.042	1.044	0.734	0.3%	0.0%
$N+M_z$ ($\theta = 60^\circ$, $\varphi = 90^\circ$)	O.I.C.	0.933	0.065	1.098	0.809	7.7%	0.0%
	EC 3	0.630	0.195	1.011	0.306	0.0%	0.0%
	A.I.S.C.	0.868	0.072	1.187	0.720	4.2%	2.3%
M_y+M_z ($\theta = 90^\circ$, $\varphi = 30^\circ$)	O.I.C.	0.984	0.072	1.200	0.771	21.2%	10.3%
	EC 3	0.850	0.188	1.035	0.435	1.3%	0.0%
	A.I.S.C.	0.813	0.108	0.929	0.386	0.0%	0.0%
M_y+M_z ($\theta = 90^\circ$, $\varphi = 60^\circ$)	O.I.C.	0.932	0.063	1.090	0.761	9.3%	0.0%
	EC 3	0.798	0.256	1.030	0.311	0.0%	0.0%
	A.I.S.C.	0.774	0.072	0.877	0.554	0.0%	0.0%
$N+M_y+M_z$ ($\theta = 30^\circ$, $\varphi = 30^\circ$)	O.I.C.	0.979	0.042	1.059	0.745	7.9%	0.0%
	EC 3	0.785	0.128	0.997	0.497	0.0%	0.0%
	A.I.S.C.	0.847	0.086	0.922	0.488	0.0%	0.0%
$N+M_y+M_z$ ($\theta = 30^\circ$, $\varphi = 60^\circ$)	O.I.C.	1.013	0.041	1.194	0.841	35.3%	1.9%
	EC 3	0.705	0.178	1.014	0.431	0.0%	0.0%
	A.I.S.C.	0.792	0.058	0.865	0.608	0.0%	0.0%
$N+M_y+M_z$ ($\theta = 60^\circ$, $\varphi = 30^\circ$)	O.I.C.	0.922	0.041	1.027	0.799	0.0%	0.0%
	EC 3	0.715	0.201	0.963	0.389	0.0%	0.0%
	A.I.S.C.	0.752	0.099	0.845	0.384	0.0%	0.0%
$N+M_y+M_z$ ($\theta = 60^\circ$, $\varphi = 60^\circ$)	O.I.C.	0.865	0.047	0.989	0.771	0.0%	0.0%
	EC 3	0.629	0.302	0.967	0.290	0.0%	0.0%
	A.I.S.C.	0.702	0.066	0.760	0.513	0.0%	0.0%

As for $N+M_y+M_z$ cases ($\theta = 60^\circ$, $\varphi = 30^\circ$, see Fig. 12), similarly to what was reported for hot-rolled sections, Eurocode 3 exhibits a dramatic discontinuity between Class 3 sections and Class 4 sections, which results in the two peaks visible on the histogram of cumulative frequencies (Fig. 12b). Results for Class 1 to 3 sections show mean values in the vicinity of 0.9, while those for Class 4 sections can only reach less than 0.7.

Oppositely, the O.I.C. performs quite well, both in terms of accuracy and consistency, as expected. Although welded sections may obviously vary more in dimensions and exhibit much more scattered patterns in resistance than hot-rolled sections, the mean value of the $\chi_{L,O.I.C.} / \chi_{L,F.E.}$ ratio can still reach a great 0.96 value with a C.O.V. as low as 7% for all of the 10 load combinations studied in this paper. It may however be noticed that for some $N+M_z$,

M_y+M_z and $N+M_y+M_z$ with dominant M_z cases, which are seldom met in practice, results of O.I.C.-based predictions may reach over 10% on the unsafe side for some very slender sections – yet maximum values are kept within 20% on the unsafe side. Shall all results, including the latter cases, be maintained safe-sided, then the accordingly-modified design proposal would lead to much more conservative predictions, overall. The authors are of the opinion that the general performance of the design proposal may not be sacrificed too much for such infrequent cases, and is therefore kept as suggested in Section 5. Given the many various section dimensions, complex section behaviour and various load situations considered, the O.I.C. is here evidenced as an excellent design proposal, significantly outperforming Eurocode 3 and A.I.S.C. specifications.

7. Conclusions

This paper investigated the cross-sectional behaviour of hot-rolled and welded I sections subjected to different combined load cases. Based on validated F.E. models, a series of numerical parametric studies were conducted to investigate the influences of manufacturing processes, yield strengths, section shapes, section slenderness and load combinations on the ultimate resistance of steel cross-sections. Based on an O.I.C. design methodology, a three-dimensional resistance surface was proposed to characterize cross-section resistance, which keeps resistance continuity from simple to combined load cases, and from stocky to slender sections. Overall, the proposed O.I.C. approach exhibited excellent resistance predictions with respect to the reference F.E. results. Also, it was shown to be significantly more accurate than the current Eurocode 3 and American Specifications design rules, which were shown to exhibit significant dispersions.

8. References

- Abaqus, G. (2011). “Abaqus 6.11:” *Dassault Systemes Simulia Corporation, Providence, RI, USA*.
- Afshan, S. and Gardner, L. (2013). “The continuous strength method for structural stainless steel design:” *Thin-Walled Structures*, Vol. 68, pp. 42–49.
- AISC (2010). ANSI/AISC 360-10 - Specification for Structural Steel Buildings, American Institute of Steel Construction, Chicago, Ill.
- ArcelorMittal Europe (2019). Sections and Merchant Bars – Sales programme.
- Arrayago, I., Rasmussen, K.J.R. and Real, E. (2017). “Full slenderness range DSM approach for stainless steel hollow cross-sections:” *Journal of Constructional Steel Research*, Vol. 133, pp. 156–166.
- Ayrton, W.E. and Perry, J. (1886). “On struts:” *The Engineer*, Vol. 62.
- Baptista, A.M. (2012). “Resistance of steel I-sections under axial force and biaxial bending:” *Journal of Constructional Steel Research*, Elsevier Vol. 72, pp. 1–11.
- Beyer, A. (2017). *On the Design of Members with Open Cross Sections Subject to Combined Axial Compression, Bending and Torsion*, PhD thesis, Lorraine University.
- Bock, M., Gardner, L. and Real, E. (2015). “Material and local buckling response of ferritic stainless steel sections:” *Thin-Walled Structures*, Vol. 89, pp. 131–141.
- Boissonnade, N., Greiner, R., Jaspart, J.-P. and Lindner, J. (2006). Rules for Member Stability in EN 1993-1-1: Background documentation and design guidelines, ECCS European Convention for Constructional Steelwork, Brussels, Belgium.
- Boissonnade, N., Hayeck, M., Saloumi, E. and Nseir, J. (2017). “An Overall Interaction Concept for an alternative approach to steel members design:” *Journal of Constructional Steel Research*, Vol. 135, pp. 199–212.
- Chen, W.-F. and Atsuta, T. (1977). *Theory of Beam Columns: In-Plane Behavior and Design*. Volume 1, J. Ross Publishing.

- Chen, Y., Cheng, X. and Nethercot, D.A. (2013). “An overview study on cross-section classification of steel H-sections:” *Journal of Constructional Steel Research*, Elsevier Vol. 80, pp. 386–393.
- EN 1993-1-1 (2005). Eurocode 3: Design of Steel Structures: Part 1-1 – General Rules and Rules for Buildings, European Committee for Standardization, Brussels, Belgium.
- EN 1993-1-5 (2006). Eurocode 3: Design of Steel Structures: Part 1-5 – Plated structural elements, Brussels, Belgium.
- Galambos, T.V. (1998). Guide to stability design criteria for metal structures, John Wiley & Sons.
- Gardner, L. (2008). “The continuous strength method:” *Proceedings of the Institution of Civil Engineers - Structures and Buildings*, Vol. 161, No. 3, pp. 127–133.
- Gérard, L. (2019). *Contribution to the design of steel I and H-sections members by means of the Overall Interaction Concept*, PhD thesis, Université Laval, Québec, Canada.
- Gérard, L., Li, L., Kettler, M. and Boissonnade, N. (2019). “Recommendations on the geometrical imperfections definition for the resistance of I-sections:” *Journal of Constructional Steel Research*, Vol. 162, p. 105716.
- Gérard, L., Li, L., Kettler, M. and Boissonnade, N. (2021). “Steel I-sections resistance under compression or bending by the Overall Interaction Concept:” *Journal of Constructional Steel Research*, Vol. 182, p. 106644.
- Gkantou, M., Theofanous, M., Wang, J., Baniotopoulos, C. and Gardner, L. (2017). “Behaviour and design of high-strength steel cross-sections under combined loading:” *Proceedings of the Institution of Civil Engineers-Structures and Buildings*, Thomas Telford Ltd Vol. 170, No. 11, pp. 841–854.
- Greiner, R., Kettler, M., Lechner, A., Freytag, B., Linder, J., Jaspart, J.P., Boissonnade, N., Bortolotti, E., Weynand, K. and Ziller, C. (2009). “SEMI-COMP: Plastic member capacity of semi-compact steel sections—a more economic design:” *European Commission, Research Fund for Coal and Steel, Luxembourg: Office for Official Publications of the European Communities*.
- Handbook of steel construction (2017). 11th Ed., Canadian Institute of Steel Construction.
- Handbook of Structural Steelwork: Eurocode edition (2013). British Constructional Steelwork Association Ltd and Steel Construction Institute.
- Hayeck, M. (2016). *Development of a new design method for steel hollow section members resistance*, PhD thesis, University of Applied Sciences of Western Switzerland - Fribourg, University of Liège, Saint-Joseph University Beirut.
- Jaspart, J.-P., Briquet, C. and Maquoi, R. (1993). Comparative study of beam-column interaction formulae. Annual Technical Session and Meeting of the SSRC.
- Johansson, B., Maquoi, R., Sedlacek, G., Müller, C. and Beg, D. (2007). “Commentary and worked examples to EN 1993-1-5 Plated Structural Elements:” *JRC scientific and technical reports*, copyright European Communities.
- Kettler, M. (2008). *Elastic-plastic cross-sectional resistance of semi-compact H- and hollow sections*, PhD thesis, Graz University of Technology, Styria, Austria.
- Kindmann, R. and Wolf, C. (2004). “Ausgewählte Versuchsergebnisse und Erkenntnisse zum Tragverhalten von Stäben aus I- und U-Profilen:” *Stahlbau*, Wiley Online Library Vol. 73, No. 9, pp. 683–692.
- Li, Y. (2014). *Extension of the Direct Strength Method to hot-rolled and welded H profile cross-sections*, PhD thesis, Université de Liège, Liège, Belgique.
- Li, L. and Boissonnade, N. (2023). “Design of mono-symmetric I-sections under combined load cases by the Overall Interaction Concept:” *Thin-Walled Structures*, Elsevier Vol. 182, p. 110280.

- Li, L., Gérard, L., Kettler, M. and Boissonnade, N. (2022a). “The Overall Interaction Concept for the design of hot-rolled and welded I-sections under combined loading:” *Thin-Walled Structures*, Vol. 172, p. 108623.
- Li, L., Gérard, L., Langlois, S. and Boissonnade, N. (2022b). “O.I.C.-based design of mono-symmetric I-sections under simple load cases:” *Thin-Walled Structures*, Vol. 174, p. 109134.
- Liang, Y., Zhao, O., Long, Y. and Gardner, L. (2019a). “Stainless steel channel sections under combined compression and minor axis bending–Part 1: Experimental study and numerical modelling:” *Journal of Constructional Steel Research*, Elsevier Vol. 152, pp. 154–161.
- Liang, Y., Zhao, O., Long, Y. and Gardner, L. (2019b). “Stainless steel channel sections under combined compression and minor axis bending–Part 2: Parametric studies and design:” *Journal of Constructional Steel Research*, Elsevier Vol. 152, pp. 162–172.
- Liang, Y., Zhao, O., Long, Y.-L. and Gardner, L. (2020). “Experimental and numerical studies of laser-welded stainless steel channel sections under combined compression and major axis bending moment:” *Thin-Walled Structures*, Elsevier Vol. 157, p. 107035.
- Liew, A. and Gardner, L. (2015). “Ultimate capacity of structural steel cross-sections under compression, bending and combined loading:” *Structures*, Vol. 1, pp. 2–11.
- Maquoi, R., Boissonnade, N., Muzeau, J.P., Jaspard, J.-P. and Villette, M. (2001). The interaction formulae for beam-columns: a new step of yet long story. SSRC Annual Technical Session and Meeting,.
- Maquoi, R. and Rondal, J. (1978). “Mise en équation des nouvelles courbes européennes de flambement:” *Construction métallique*, Vol. 15, No. 1, pp. 17–30.
- Massonnet, C. (1976). “Forty years of research on beam-columns in steel:” *Solid Mechanics Archives*, Noordhoff International Publishing Leyden Vol. 1, No. 1, pp. 27–157.
- Nseir, J. (2015). *Development of a new design method for the cross-section capacity of steel hollow sections*, PhD thesis, Université de Liège, Liège, Belgique.
- Ofner, R. (1997). Traglasten von stäben aus stahl bei druck und biegun, Techn. Univ.
- Rasmussen, K.J. (2006). “Design of slender angle section beam-columns by the direct strength method:” *Journal of Structural Engineering*, American Society of Civil Engineers Vol. 132, No. 2, pp. 204–211.
- Rubin, H. (1978). “Interaktionsbeziehungen für doppelsymmetrische I- und Kasten-Querschnitte bei zweiachsiger Biegung und Normalkraft:” Vol. 47, pp. 145–181.
- Schafer, B.W. (2008). “Review: The Direct Strength Method of cold-formed steel member design:” *Journal of Constructional Steel Research*, Vol. 64, No. 7–8, pp. 766–778.
- Steel Construction Manual (2017). 15th Ed., American Institute of Steel Construction.
- Sun, Y., Su, A., Jiang, K., Liang, Y. and Zhao, O. (2021). “Testing, numerical modelling and design of stainless steel welded I-sections under minor-axis combined loading:” *Engineering Structures*, Elsevier Vol. 243, p. 112513.
- Torabian, S. and Schafer, B.W. (2018). “Development and experimental validation of the direct strength method for cold-formed steel beam-columns:” *Journal of Structural Engineering*, American Society of Civil Engineers Vol. 144, No. 10, p. 04018175.
- Yuan, H.X., Wang, Y.Q., Gardner, L., Du, X.X. and Shi, Y.J. (2015). “Local–overall interactive buckling behaviour of welded stainless steel I-section columns:” *Journal of Constructional Steel Research*, Vol. 111, pp. 75–87.
- Yun, X. and Gardner, L. (2017). “Stress-strain curves for hot-rolled steels:” *Journal of Constructional Steel Research*, Vol. 133, pp. 36–46.
- Yun, X., Gardner, L. and Boissonnade, N. (2018a). “Ultimate capacity of I-sections under combined loading–Part 1: Experiments and FE model validation:” *Journal of Constructional Steel Research*, Elsevier Vol. 147, pp. 408–421.

- Yun, X., Gardner, L. and Boissonnade, N. (2018b). “Ultimate capacity of I-sections under combined loading–Part 2: Parametric studies and CSM design:” *Journal of Constructional Steel Research*, Elsevier Vol. 148, pp. 265–274.
- Yun, X., Gardner, L. and Boissonnade, N. (2018c). “The continuous strength method for the design of hot-rolled steel cross-sections:” *Engineering Structures*, Vol. 157, pp. 179–191.
- Zhao, O., Afshan, S. and Gardner, L. (2017). “Structural response and continuous strength method design of slender stainless steel cross-sections:” *Engineering Structures*, Vol. 140, pp. 14–25.
- Zhao, O., Rossi, B., Gardner, L. and Young, B. (2015a). “Behaviour of structural stainless steel cross-sections under combined loading–Part I: Experimental study:” *Engineering Structures*, Elsevier Vol. 89, pp. 236–246.
- Zhao, O., Rossi, B., Gardner, L. and Young, B. (2015b). “Behaviour of structural stainless steel cross-sections under combined loading–Part II: Numerical modelling and design approach:” *Engineering Structures*, Elsevier Vol. 89, pp. 247–259.